steel research international

Microstructure and Texture of Strip Cast Grain-Oriented Silicon Steel after Symmetrical and Asymmetrical Hot Rolling

Hong-Yu Song, Hui-Hu Lu, Hai-Tao Liu,* Hao-Ze Li, Dian-Qiao Geng, R. Devesh K. Misra, Zhen-Yu Liu, and Guo-Dong Wang

A grain-oriented silicon steel as-cast strip was produced by twin-roll strip casting. Then the as-cast strip was symmetrically and asymmetrically hot rolled, respectively. The microstructure and texture evolution was investigated by a combination of optical microscopy, X-ray diffraction, and electron backscattered diffraction methods. The microstructure of the as-cast strip consisted of ferrite matrix and martensite, and the texture was characterized by pronounced {001} ⟨0vw⟩ fiber texture in the outer layers and nearly random texture in the inner layers. After symmetric hot rolling, the microstructure was composed of deformed ferrite grains, proeutectoid ferrite grains and pearlite. The texture was characterized by pronounced {001} ⟨0vw⟩ fiber texture in the outer layers and mild γ-fiber texture in the inner layers. By contrast, when asymmetric hot rolling was applied, considerably dispersive proeutectoid ferrite and pearlite and relatively strong Goss texture were observed, together with strong {001} ⟨0vw⟩ fiber texture in the outer layers.

1. Introduction

Grain-oriented silicon steels are important soft magnetic materials widely used for transformer cores.[1,2] Although the manufacturing process has been well established since Goss[3] first proposed the technological route in 1934, the conventional process is still complicated.[4] The progress in strip casting technology provides a possibility of producing silicon steels by a simpler process than conventional process.[5,6] Strip casting technology can eliminate the thick slab casting and reduce hot rolling passes by supplying as-cast strips with thickness close to the conventional hot rolled sheets directly from the melt.[7–10] Thus, the microstructure and texture of the strip-cast strips significantly differ from those of the conventional casting slab and hot rolled sheets. Park et al.[5] investigated the microstructure, texture and deformation behavior of strip-cast 4.5 wt% Si steel along the thickness direction. More recently, Liu et al.[11–14] clarified the microstructure and texture evolution of twin roll strip-cast 3 wt% Si non-oriented steel and 6.2 wt% Si steel. By contrast, grain-oriented silicon steels experience incomplete γ/α phase transformation during casting and subsequent cooling stage. Thus, the microstructure and texture evolution of strip-cast grain-oriented silicon steel is different from the studied steels by the above-mentioned researchers. However, the corresponding studies have not yet been reported.

It is known that the {110} ⟨001⟩ orientation (Goss texture) in the hot rolled sheet has an important influence on the nucleation of {110} ⟨001⟩ secondary grains by way of structure memory[15] even after the cycle of normalization, cold rolling and subsequent annealing. The origination of Goss texture in conventional process is attributed to the severe shear deformation during hot rolling in which the thickness reduction usually exceeds 90%.[16] By contrast, given that the thickness of the as-cast strip is close to that of the final hot rolled strip, so small hot rolling reduction may restrict the origination of Goss texture due to the lack of shear deformation. Studies indicated that asymmetric rolling can generate an additional shear deformation and resulted in intense shear texture through the whole sheet thickness.[17,18] Asymmetric cold rolling was carried out in aluminum alloys[19] and pure aluminum[20] for modifying texture. Liu et al.[21] applied

[*] H.-Y. Song, H.-H. Lu, H.-T. Liu, H.-Z. Li, Z.-Y. Liu, G.-D. Wang
State Key Laboratory of Rolling and Automation, Northeastern University, Shenyang 110819, China
Email: Liuht@ral.neu.edu.cn
D.-Q. Geng
Key Laboratory of National Education Ministry for Electromagnetic Processing of Materials, Northeastern University, Shenyang 110819, China
R. D. K. Misra
Department of Chemical Engineering, Center for Structural and Functional Materials, University of Louisiana at Lafayette, LA 70504-4130, USA

DOI: 10.1002/srin.201300385

asymmetric cold rolling to the grain-oriented silicon steels produced by conventional casting with the concern about producing thin gauge sheets. However, the effect of asymmetric hot rolling (ASHR) on microstructure and texture of strip-cast grain-oriented silicon steel has not yet been reported.

In the present work, an as-cast grain-oriented steel strip was produced by twin-roll strip casting and followed by symmetric hot rolling (SHR) and ASHR, respectively. The goal of this paper is to clarify the microstructure and texture evolution of as-cast and hot rolled strips.

2. Experimental Procedure

A grain-oriented silicon steel (Si 3.1, C 0.066, Mn 0.16, S 0.013, P 0.01, mass%) as-cast strip with 3.6 mm was produced by twin-roll strip casting, as described in detail earlier by Liu et al.[11–14] The melt superheat in the pool was controlled to be 40°C. Then, the as-cast strips were heated to 1150°C and hot rolled in two passes with a total reduction of 35% using SHR and ASHR mills, respectively, and air-cooled to room temperature. The mismatch speed ratio of ASHR in this study was 1.39 and the lower roll had higher velocity (0.10 m s^{-1}). In this paper, the strip surface in contact with the lower roll was defined as lower surface, while the other surface was referred as the upper surface.

Specimens were etched with 4% nital for metallographic examination. The microstructure was observed with a LEICA-DMIRM optical microscope. The orientation image maps of the strips were determined by the electron backscatter diffraction (EBSD) system equipped at Zeiss Scanning Electron Microscope. The orientation distribution functions (ODFs) of the strips were measured and calculated at different thickness layers using a Bruker D8 Discover X-ray Diffractometer. The samples used for texture measurements were prepared with the size of 22 mm (L) × 20 mm (W). The position through the thickness direction can be defined by a parameter s, as $s = 2a/d$, where a and d were the distance from the center layer and the sheet thickness, respectively. For ASHR strips, the upper surface, the center and the lower surface were respectively defined as $s = 1$, $s = 0$, and $s = -1$.

3. Results

3.1. Microstructure and Texture of As-Cast Strip

Figure 1 shows the microstructure of the as-cast strip. It was observed that the microstructure consisted of large ferrite grains and lots of needle-shaped or island-shaped martensite. The ferrite matrix was characterized by a mixture of outer columnar grains and inner equiaxed grains. **Figure 2** shows the texture at different layers of the as-cast strip. The texture was characterized by pronounced {001} ⟨0vw⟩ fiber in the outer layers and nearly random texture in the inner layers.

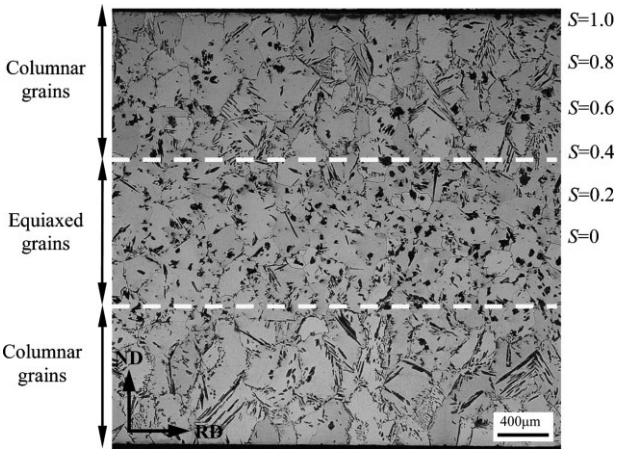

Figure 1. Optical microstructure of as-cast strip (longitudinal section).

3.2. Microstructure and Texture of Hot Rolled Strips

Figure 3 shows the microstructure of the hot rolled strips. The microstructure in the SHR strip was characterized by deformed ferrite grains, proeutectoid ferrite grains, and pearlite (Figure 3a and b). By contrast, considerably dispersive proeutectoid ferrite and pearlite in the ASHR strip was observed (Figure 3c). Besides, an amount of banded structures indicated by dotted ellipses were observed. Figure 3d shows the optical microscopy of these banded structures at higher magnification. The deviation degrees of the banded structures from the rolling direction were 30°–45°. Fine and dispersive proeutectoid ferrite and pearlite were found in the banded structures.

Figure 4 shows the texture at various layers of the SHR strip. The texture was characterized by pronounced {001} ⟨0vw⟩ fiber texture in the outer layers and mild γ-fiber

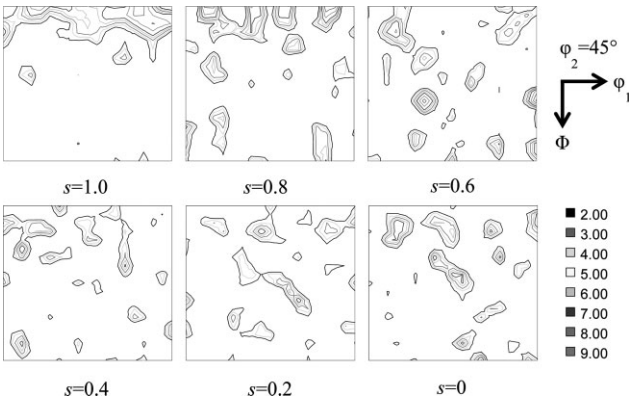

Figure 2. Textures in various thickness layers of the as-cast strip.

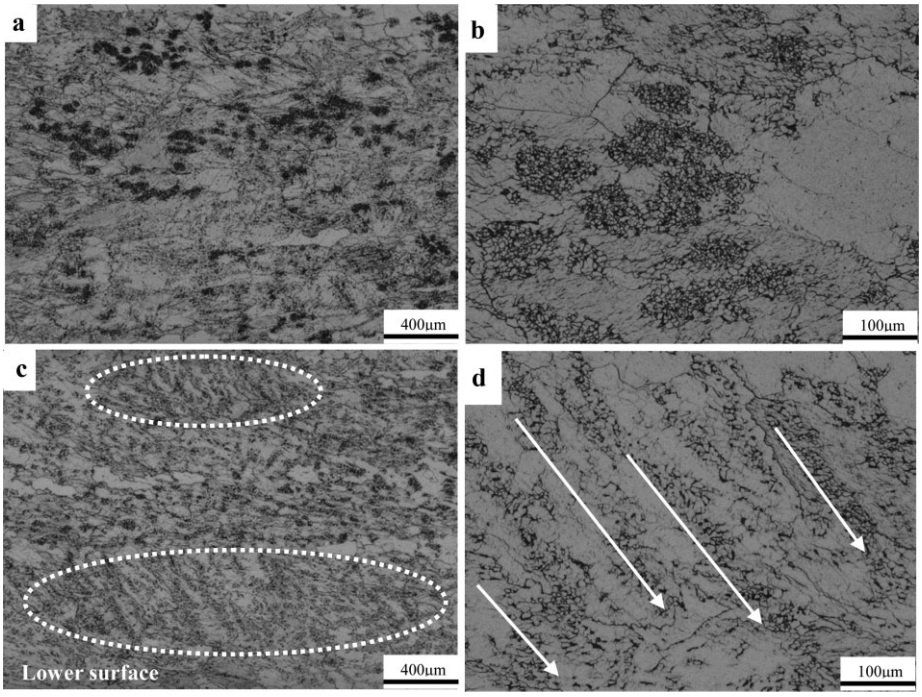

Figure 3. Low a) and high b) magnification microstructure of symmetrically hot rolled strip, and low c) and high d) magnification microstructure of asymmetrically hot rolled strip.

texture in the inner layers. **Figure 5** shows the texture variation from the lower surface to the center layer of the ASHR strip. Strong {001} ⟨0vw⟩ fiber texture was observed in the outer layers and very weak texture evolved in the inner layers. It should be noted that relatively strong Goss texture at layer $s=-0.8$, $s=-0.2$, and $s=-0.1$ were observed with the intensity of 3.63 times, 3.06 times, and 3.81 times of random distribution, respectively. **Figure 6** shows the effects of SHR and ASHR on the intensities of Goss texture through the thickness. It was

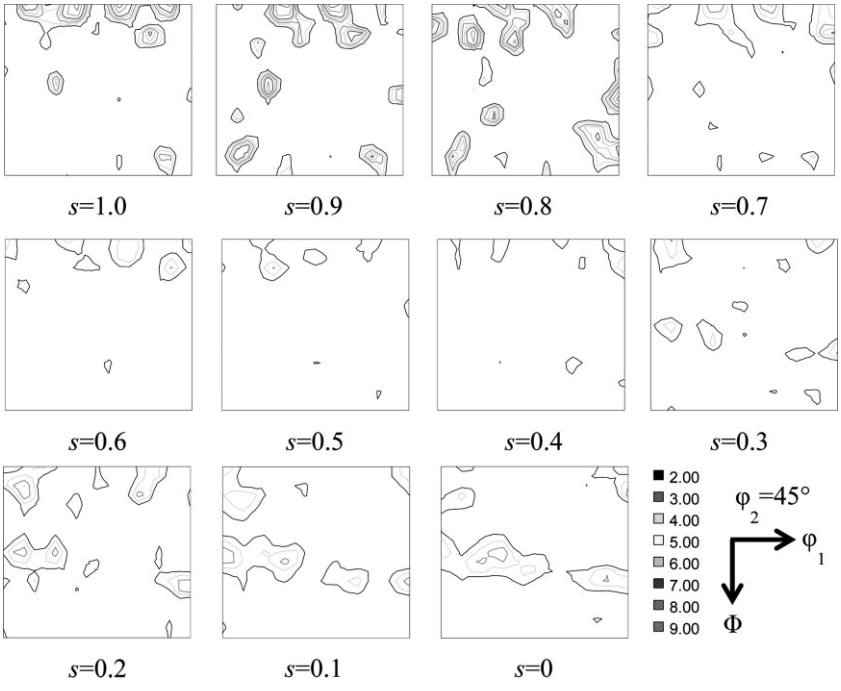

Figure 4. Textures in various thickness layers of symmetrically hot rolled strip.

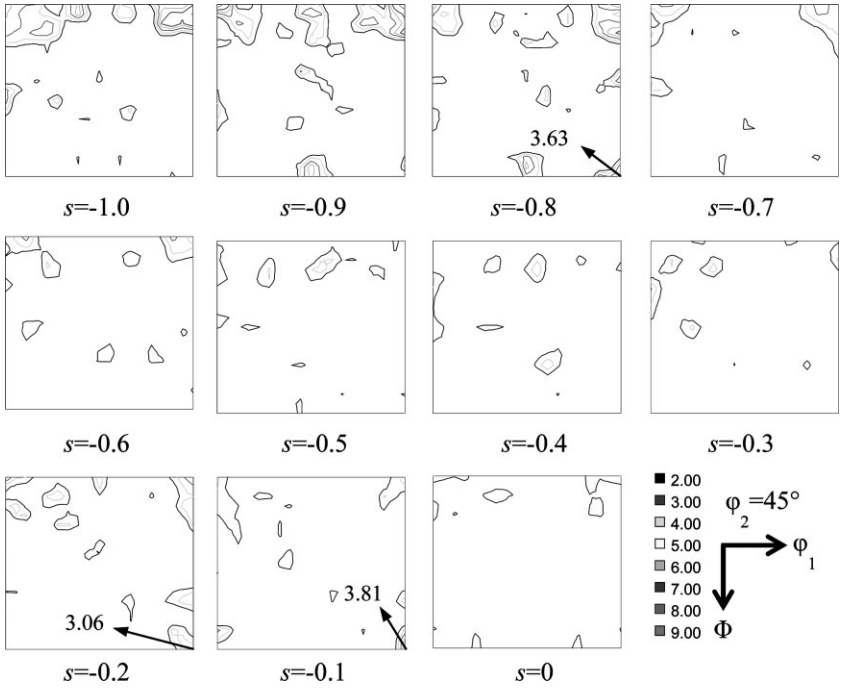

Figure 5. Textures in various thickness layers of asymmetrically hot rolled strip.

observed that the intensity of Goss texture fluctuated sharply along the thickness direction in both SHR and ASHR strips. The Goss texture in the SHR strip was very weak through the thickness. By contrast, the Goss texture was greatly enhanced in the ASHR strip, though it was still very weak at some layers.

Figure 7a and b shows the EBSD micrographs of the SHR and ASHR strip, respectively. The Goss grains were indicated by the dotted ellipses. The Goss grains in SHR strip were mainly observed near the subsurface i.e. $s = 0.8$ to $s = 0.6$. By contrast, more Goss grains were observed in the ASHR strip and some Goss grains were evolved at deep layers. Furthermore, a banded distribution of Goss grains can be found in the ASHR strip, which was in good agreement with the banded structure shown in Figure 3c and d.

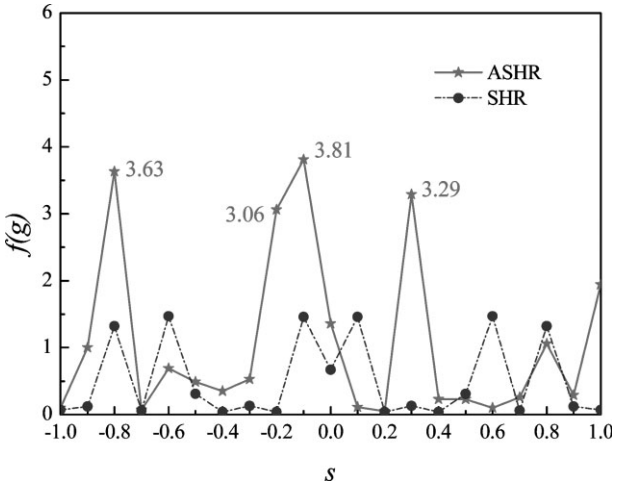

Figure 6. Intensity of Goss orientation of symmetrically and asymmetrically hot rolled strips through the sheet thickness.

4. Discussion

4.1. Microstructure and Texture Evolution in As-Cast Strip

Liu et al.[11] confirmed that the melt superheat in the pool can affect the temperature gradient in front of the solid phase during strip casting. So the melt superheat was the most important factor to determine solidification microstructure. When the melt superheat was relatively high, such as 40°C in the present work, the temperature gradient in front of the solid phase could satisfy the selective growth mechanism for some {001} columnar δ-ferrite grains at the early stage of solidification. The columnar grains of the as-cast strip in this study were observed between $s = 1.0$ layer and $s = 0.5$ layer. However, with the growth of {001} columnar δ-ferrite grains, the temperature gradient decreased and the selective growth effect vanished at the end of solidification, thus gave rise to the formation of the equiaxed δ-ferrite grains in the center. During the air-cooling stage after solidification, a fraction of δ-ferrite transformed into austenite and subsequently transformed into martensite due to the relatively high cooling rate. Thus, the martensite inherited the morphology of parent austenite. The needle-shaped and island-shaped austenite occurred in the present study was quite similar to the

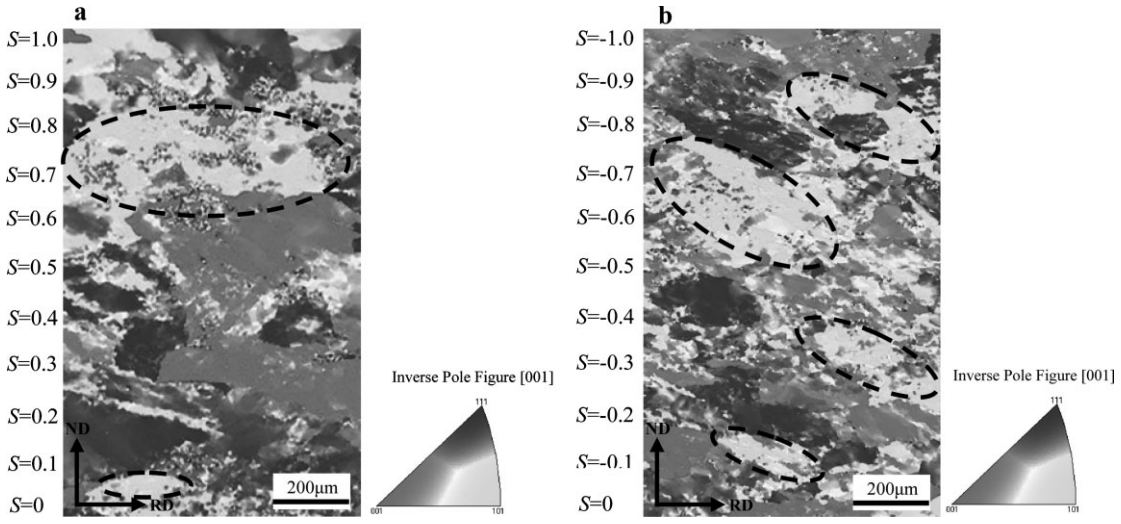

Figure 7. EBSD micrographs of a) symmetrically and b) asymmetrically hot rolled strip.

Widmanstätten and allotriomoph austenite existed in low carbon steel, in which it was reported that a well-developed Widmanstätten structure tended to be formed at a high cooling rate such as $40\,^{\circ}C\,s^{-1}$.[22] Obviously, in the present study, the Widmanstätten austenite formed near the surface was attributed to a relatively higher cooling rate, while the allotriomoph austenite formed in the center was due to a relatively lower cooling rate.

It is known that the Widmanstätten austenite obeys the Kurdjumov–Sachs (K–S) relationship with respect to the parent ferrite,[23,24] while the allotriomoph austenite has no specific orientation relationship with parent ferrite. Then the lath martensite obeys the K–S or Nishiyama–Wasserman (N–W) orientation relationship with parent austenite during transformation.[25,26] However, in the present work, the volume fraction of martensite was only about 13% in the as-cast strip due to the very limited $\delta \rightarrow \gamma$ transformation. Consequently, the transformation type textures were negligible and the texture of the as-cast strip was characterized by the orientations of the initial solidification δ-ferrite. As a result, considering the solidification microstructure through the thickness (Figure 1), it could be inferred that the {001} ⟨0vw⟩ fiber texture in the out layers and the nearly random texture in the center layers were mainly attributed to the formation of outer columnar δ-ferrite grains and inner equiaxed δ-ferrite grains, respectively.

4.2. Microstructure and Texture Evolution in SHR and ASHR Strips

When the as-cast strip was heated to 1150°C and hot rolled, the microstructure consisted of ferrite and austenite. During the air-cooling stage, firstly partial austenite was transformed into proeutectoid ferrite below A_3 temperature and subsequently the rest of austenite was transformed into pearlite below A_1 temperature. Specially, ASHR could cause larger shear deformation through the whole strip compared with SHR. In the case of ASHR, the austenite grains suffered severe deformation and were elongated, and finally led to dispersive proeutectoid ferrite and pearlite after $\gamma \rightarrow F + P$ transformation. Therefore, the proeutectoid ferrite and pearlite showed a more dispersive distribution in ASHR strip than those in SHR strip (Figure 3). The improvement of microstructure homogeneity is very helpful to obtain dispersed inhibitors such as AlN and MnS.

As shown in Figure 6, the Goss texture of the ASHR strip was relatively stronger than that of the SHR strip. It is known that the origination of Goss texture in grain-oriented silicon steel is as a result of the shear deformation during hot rolling.[15,16,27,28] In the present work, during SHR, shear deformation occurred due to the high friction between the roll and as-cast strip surface and was restricted to the region from the sheet surface to one-fourth thickness. Therefore, Goss texture mainly evolved between $s = 0.8$ layer and $s = 0.6$ layer (Figure 6 and 7a), in good agreement with the observation in the conventional hot rolled sheet from thick slab. However, it should be noted that Goss texture in SHR sheet was much weaker in comparison with that in the conventional hot rolled sheet due to the relatively small hot rolling reduction. By contrast, during ASHR, a velocity ratio as high as 1.39 could lead to a severe shear deformation through the whole strip[29] in addition to the shear deformation caused by the high friction between the roll and as-cast strip surface. Consequently, relatively stronger Goss texture was evolved in ASHR strip (Figure 6 and 7b). Exceptionally, because the surface strong columnar ferrite grains with {001} ⟨0vw⟩ orientations were hard to rotate into Goss orientation during hot rolling, the Goss texture was relatively weaker on the surface of both SHR and ASHR strips. To be interesting, the intensity of Goss texture

exhibited a few peaks through the thickness in both SHR and ASHR samples (Figure 6). This may be related with the complex shear deformation distribution along thickness direction during two-pass hot rolling which was different from that during single-pass hot rolling. However, the interesting phenomenon should be paid great attention in the future.

5. Conclusions

A grain-oriented silicon steel as-cast strip was produced by twin-roll strip casting and followed by the symmetric and ASHR, respectively. The microstructure and texture evolution of the as-cast strip and hot rolled strips was investigated. The conclusions are summarized as follows:

1. The microstructure of the as-cast strip was composed of ferrite and martensite, and the texture was characterized by pronounced {001} ⟨0vw⟩ fiber texture in the outer layers and nearly random texture in the inner layers.
2. The hot rolled microstructure and texture can be changed by applying different rolling methods. The microstructure of the symmetrically hot rolled strip consisted of deformed ferrite grains, proeutectoid ferrite grains and perlite, and the texture revealed strong {001} ⟨0vw⟩ fiber texture in the outer layers and mild γ fiber texture in the inner layers.
3. Considerably dispersive proeutectoid ferrite and pearlite and relatively stronger Goss texture were observed in the asymmetrically hot rolled strip.

Acknowledgements

The authors gratefully acknowledge the financial supports from National Natural Science Foundation of China (Grant nos. 50734001, 51004035, 51174059, 51374002) and the Fundamental Research Funds for the Central Universities (Grant no. N120407009).

Received: October 15, 2013

Keywords: strip casting; grain-oriented silicon steel; asymmetric hot rolling; microstructure; texture

References

[1] V. Stoyka, F. Kováč O. Stupakov, I. Petryshynets, *Mater. Charact.* **2010**, *61*, 1066.
[2] T. Kubota, M. Fujikura, Y. Ushigami, *J. Magn. Magn. Mater.* **2000**, *215–216*, 69.
[3] N. P. Goss, U. S. Patent 1965559 1934.
[4] D. Senk, C. Schneider, R. Kopp, *Steel Times Int.* **1991**, *14*, 46.
[5] J. Y. Park, K. H. Oh, H. Y. Ra, *ISIJ Int.* **2000**, *40*, 1210.
[6] H. Litterscheidt, R. Hammer, C. Schneider, R. W. Simon, D. Senk, R. Kopp, B. Hehl, *Stahl Eisen.* **1991**, *111*, 61.
[7] A. R. Buchner, J. W. Schmitz, *Steel Res.* **1992**, *63*, 7.
[8] J. C. Grosjean, J. L. Jacquo, J. M. Damasse, H. Literscheidt, D. Senk, W. Schmitz, *Iron Making Steel Making* **1993**, *20*, 27.
[9] D. Raabe, *Acta Metall. Mater.* **1997**, *45*, 1137.
[10] J. Y. Park, K. H. Oh, H. Y. Ra, *Scr. Mater.* **1999**, *40*, 881.
[11] HT. Liu, Z. Y. Liu, C. G. Li, G. M. Cao, G. D. Wang, *Mater. Charact.* **2011**, *62*, 463.
[12] H. T. Liu, Z. Y. Liu, G. M. Cao, C. G. Li, G. D. Wang, *J. Magn. Magn. Mater.* **2011**, *323*, 2648.
[13] H. T. Liu, Z. Y. Liu, Y. Sun, Y. Q. Qiu, C. G. Li, G. M. Cao, B. D. Hong, S. H. Kim, G. D. Wang, *Mater. Lett.* **2012**, *81*, 65.
[14] H. T. Liu, Z. Y. Liu, Y. Q. Qiu, Y. Sun, G. D. Wang, *J. Mater. Process. Technol.* **2012**, *212*, 1941.
[15] Y. Shimizu, Y. Ito, Y. Iida, *Metall. Trans. A.* **1986**, *17A*, 1323.
[16] M. Matsuo, *ISIJ Int.* **1989**, *29*, 809.
[17] S. H. Kim, B. S. You, C. D. Yim, Y. M. Seo, *Mater. Lett.* **2005**, *59*, 3876.
[18] S. H. Lee, D. N. Lee, *Int. J. Mech. Sci.* **2001**, *43*, 1997.
[19] H. Jin, D. J. Lloyd, *Mater. Sci. Eng. A* **2005**, *399*, 358.
[20] K. H. Kim, D. N. Lee, *Acta Mater.* **2001**, *49*, 2583.
[21] G. Liu, F. Wang, L. Zuo, K. M. Qi, Z. D. Liang, *Scr. Mater.* **1997**, *37*, 1877.
[22] N. H. Pryds, X. Huang, *Metall. Trans. A.* **2000**, *31A*, 3155.
[23] K. Ameyama, G. C. Weatherly, K. T. Aust, *Acta Metall. Mater.* **1992**, *8*, 1835.
[24] C. H. Shek, C. Dong, J. K. L. Lai, K. W. Wong, *Metall. Trans. A.* **2000**, *31A*, 15.
[25] S. Morito, H. Tanaka, R. Konishi, T. Furuhara, T. Maki, *Acta Mater.* **2003**, *51*, 1789.
[26] G. Miyamoto, N. Iwata, N. Takayama, T. Furuhara, *Acta Mater.* **2010**, *58*, 6393.
[27] W. Truszkowski, J. Krol, B. Major, *Metall. Trans.* **1980**, *11A*, 749.
[28] W. Truszkowski, J. Krol, B. Major, *Metall. Trans.* **1982**, *13A*, 665.
[29] F. Zhang, G. Vincent, Y. H. Sha, L. Zuo, J. J. Fundenberger, C. Esling, *Scr. Mater.* **2004**, *50*, 1011.